Ninth Symposium on Global Change Studies, Preprint Vol., Amer. Meteor. Sot., Boston, 1998, in press.

2.6 EXTRATROPICAL INFLUENCE OF UPPER TROPOSPHERIC WATER VAPOR ON GREENHOUSE WARMING

Hua Hu* and W. Timothy Liu
Jet Propulsion Laboratory, Pasadena, California

1. INTRODUCTION

Despite its small quantity, the importance of upper tropospheric water vapor is its ability to trap the longwave radiation emitted from the Earth's surface, namely the greenhouse effect. The greenhouse effect is defined quantitatively as the difference between the longwave flux emitted by the Earth's surface and the outgoing longwave radiation (OLR) flux emitted from the top of the atmosphere (TOA) (Raval and Ramanathan 1989). A recent study by **Soden and** Fu (1995) examined the relationship between the upper tropospheric relative humidity, greenhouse effect, and deep convection, and found a positive correlation between these **three quantities** for both spatial and temporal variations in Tropics, but little relationship between upper tropospheric relative humidity and greenhouse effect in extratropical regions. The reported upper tropospheric relative humidity field was retrieved from infrared channel at 6.7pm on TIROS Operational Vertical Sounder (TOVS) platform. We speculated that the relative humidity field is not a sufficient surrogate to represent the upper tropospheric moisture in extratropics due to the large spatial and temporal variations in the upper air temperature in these regions. The purpose of this paper is to re-examine the impact of upper tropospheric water vapor on greenhouse warming in midlatitudes by analyzing the recent observations of the upper tropospheric water vapor from the Microwave Limb Sounder (MLS) on the Upper Atmosphere Research Satellite (UARS), in conjunction with other space-based measurements and model simulation products.

The UARS MLS has taken direct measurements of water vapor content at pressure levels at 464 mb, 315 mb, 215 mb, and 146 mb since late September 1991 until present (with associated interruptions). The advantages of MLS over other instruments are the ability to observe through thin cloud-like cirrus and a better vertical resolution of 3 km than the 6.7 μm product (Read et al. 1995).

This paper combined observations from several independent space-based instruments to study the relation of upper tropospheric water vapor to climate. First, a summary of data sets is presented in section 2. Then a relationship of upper tropospheric water vapor and greenhouse effect in the extratropical area is shown in section 3. It is noted that in Northern Hemisphere midlatitudes, both the upper tropospheric water vapor and the greenhouse effect reaches its maximum along storm tracks in the North Pacific and Atlantic. The possible mechanism of maintaining the upper tropospheric moisture in extratropical areas is also discussed in section 3.

2. DATA

The best sensitivity of MLS instrument to water vapor is at -12 km height at low latitudes and -7 km height at high latitudes. Therefore, for midlatitude studies, we use the MLS water vapor measurements at pressure level 215 mb and 315 mb. The data were monthly averaged to a 2.5° latitude by 2.5° longitude grid. Because the UARS satellite yawed 180 degrees every 36 days, so the mid and high latitude coverages alternate between Northern Hemisphere and Southern Hemisphere every 36 days.

The normalized greenhouse effect was calculated from $g = (\sigma T_s^4 - F) / (\sigma T_s^4)$, where T_s is the

*Corresponding author address: Dr. Hua Hu, Earth and Space Sciences Division, M/S 300-323, Jet Propulsion Laboratory, 4800 Oak Grove Drive, Pasadena, CA 91 108;
e-mail: hxh@pacific.jpl.nasa.gov

surface temperature, F is the OLR flux at the top of the atmosphere, and σ is the Stephan-Boltzman constant. The OLR observations were obtained by the nonscanner instrument in the Earth Radiation Budget Experiment (Luther et al. 1986). The sea surface temperature (SST) data were derived by Advanced Very High Resolution Radiometer (AVHRR) blended within situ measurements (Reynolds and Smith 1995).

The deep convection cloud amount represents the fractional area coverage of those high clouds which have cloud top pressure less than 440 mb and optical thickness greater than 22.63. The deep convection cloud information was provided from the International Satellite Cloud Climatology Project (ISCCP) D2 monthly mean data set (Rossow and Schiffer 1991).

Since most water vapor in the atmosphere is constrained in the lower troposphere, the total precipitable water observed from Special Sensor Microwave Image (SSM/I) can be considered approximately equal to the water content in the lower troposphere, and was compared with MLS upper tropospheric water vapor measurements in this study. Re-analysis data produced by Goddard Earth Observing System - Data Assimilation System (GEOS- DAS) were used to study baroclinic activity in midlatitudes.

3. OBSERVATION AND **DISCUSSION**

The impact of upper tropospheric water vapor on the greenhouse effect in Northern Hemisphere midlatitudes is presented here using measurements from monthly mean in July 1992 on a 2.5° latitude and 2.5° longitude grid. Data shown in the top and middle panels in Figure 1 were taken from independent space-based instruments MLS, ERBE, and AVHRR. The bottom panel of Figure 1 is the model simulated water vapor produced by the GEOS-DAS project. In contrary to the geographic distribution of the upper tropospheric relative humidity which increases with latitude in extratropical regions (Soden and Fu 1995), the MLS upper tropospheric specific humidity measurements at 315 mb have high values along storm tracks in Pacific and Atlantic, superimposed on a background distribution which has magnitude decreasing with latitude. The enhancement of upper tropospheric water vapor along storm tracks is collocated with an increase in greenhouse warming, as shown in the middle panel of Figure 1, clearly demonstrating the role of the upper tropospheric humidity in trapping longwave radiation. The distribution of upper tropospheric humidity derived from the GEOS-DAS model simulation (the bottom panel of Figure 1) does not resemble the UARS MLS observations in respect to the fine structure along storm tracks. It agrees more with the surface temperature distribution (the bottom panel of Figure 3) and may imply a deficiency in model simulation of upper atmosphere hydrologic balance. One possible explanation is that the model does not have a sufficient spatial resolution in respect to both the horizontal and vertical directions in simulating large gradients in water vapor distributions.

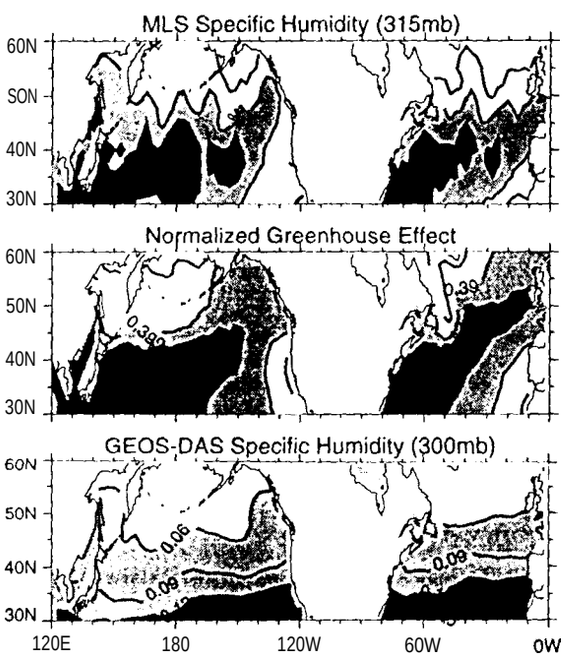

FIG. 1. Top panel is the geographic map of the UARS MLS upper tropospheric water vapor measurements at 315 mb, contour interval is 0.05 g/kg, values greater than 0.23 g/kg and 0.28 g/kg are denoted by light and dark shading, respectively. The middle panel is the normalized greenhouse effect, contour interval is 0.03, values greater than 0.39 and 0.42 are denoted by light and dark shading, respectively. The bottom panel is the model simulated specific humidity at 300 mb from the GEOS-DAS re-analysis data, contour interval is 0.03 g/kg, values greater than 0.06 g/kg and 0.12 g/kg are denoted by light and dark shading, respectively. Data are monthly average in July 1992.

The deep convection cloud coverage from ISCCP is shown in the top panel of Figure 2, indicating that the increased amount of deep convective clouds along storm tracks transports more water vapor upward to the tropopause. The analysis of wind field data derived from GEOS-DAS re-analysis

data product demonstrated that the generation of these deep convective clouds is associated with synoptic-scale baroclinic waves along storm tracks. The baroclinic activity is measured with the baroclinicity index, namely, the maximum Eady growth rate (Lindzen and Farrell 1980), as shown in the bottom panel of Figure 2. The baroclinicity index was calculated from $\sigma_{BI}=0.31|\partial U/\partial Z|$ N-I using GEOS-DAS wind field at 850 mb and 700 mb levels, where f is the Coriolis parameter, $\partial U/\partial Z$ is the zonal wind vertical shear, and N is the Brunt-Väisälä frequency. Higher baroclinicity index indicates higher eddy activity. Hoskins and Valdes (1990) showed that high baroclinicity over the winter Northern Hemisphere is located along storm track regions. Del Genio et al. (1994) used a general circulation model (GCM) to study the maintenance of the upper tropospheric water vapor distribution and argued that the eddies play an important role in moistening the extra tropical upper troposphere. Baroclinic wave features were also observed in MLS upper tropospheric water vapor in extratropical Southern Hemisphere summertime (Elson et al. 1996; Stone et al. 1996).

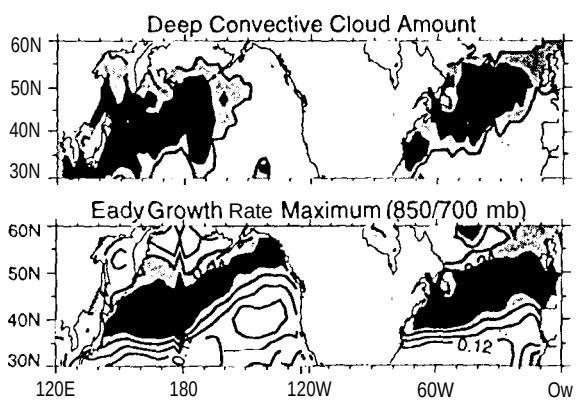

FIG. 2. The top panel is the fractional area coverage of deep convection cloud from ISCCP D2 monthly average in July 1992, contour interval is 2%, values greater than 2% and 4% are denoted by light and dark shading, respectively. The bottom panel is the calculated Eady growth rate maximum for the 850-700 mb layer using GEOS-DAS re-analysis data, contour interval is 0.04 day"', values large than 0.2 day-' and 0.24 day"' in magnitude are denoted by light and dark shading, respectively.

Since the greenhouse effect is sensitive to surface temperature and vertical structure of water vapor content, it is important to know the relative contribution of each component. The distribution of vertical integrated water vapor which is mostly constrained in the lower troposphere (the top panel of Figure 3) closely follows sea surface temperature (the bottom panel of Figure 3) and is less zonally oriented than the greenhouse effect and the upper tropospheric water vapor, reflecting the fact that the upper tropospheric water vapor contributes more than the lower tropospheric water vapor toward trapping the infrared radiation in the extratropical areas. Also, it is shown in Figures 2 and 3 that the extratropical upper tropospheric water vapor is likely to be governed by the large-scale dynamics and not the local temperature, in contrary to some popular postulations for tropical areas.

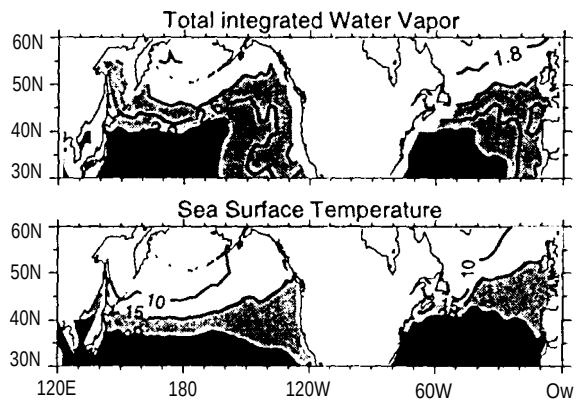

FIG. 3. The top panel is the total integrated water vapor from SSM/I measurements, contour level is 0.4 g/cm2, values greater than 2.2 g/cm2 and 3.0 g/cm2 are denoted by light and dark shading, respectively. The bottom panel is the sea surface temperature from AVHRR, contour level is 50C, values greater than 150C end 200C are denoted by light and dark shading, respectively. Data are monthly average in July 1992.

4. SUMMARY

Although the upper tropospheric water vapor content in the extratropical regions is much smaller than that in the Tropics and in the lower troposphere, the analysis of MLS upper tropospheric water vapor measurements reveals its importance of trapping the Earth's radiation. It is found that the MLS upper tropospheric water vapor enhances along storm tracks in North Pacific and Atlantic, collocating with an increase in greenhouse warming along storm tracks. The mechanism of enhanced upper tropospheric humidity along storm tracks seems to be associated with the increased amount of deep convective cloud which transports water vapor upward to the tropopause. The analysis of data derived from a general circulation model indicated that the generation of these deep convective clouds is associated with synoptic-scale baroclinic

waves along storm tracks. By comparing with the sea surface temperature, it indicates that the upper tropospheric water vapor, unlike the lower tropospheric water vapor, is likely governed by the large-scale dynamics and not the local temperature.

Acknowledgment. The authors would like to thank Drs. Joe Waters and Bill Read in MLS group for providing the MLS upper tropospheric water vapor data. This study was conducted at the Jet Propulsion Laboratory, California Institute of Technology, under contract with the National Aeronautics and Space Administration (NASA) This research was supported by the NASA Earth Observing System (EOS) Interdisciplinary Science Investigation.

REFERENCES

Elson, L. S., W. G. Read, J. W. Waters, P. W. Mote, J. S. Kinnersley and R.S. Harwood, 1995: Space-time variations in water vapor as observed by the UARS Microwave Limb Sounder. *J. Geophys. Res.,* 101,9001-9016.

Hokins, B. J., and P. J. Valdes, 1990: On the existence of storm tracks. *J. Atmos. Sci.,* 47, 1854-1864.

Lidzen, R. S., and B. Farrell, 1980: A simple approximate result for the maximum growth rate of baroclinic instabilities. *J. Atmos. Sci.,* 37, 1648-1654.

Luther, M. R., J. E. Cooper, and G. R. Taylor, 1986: The earth radiation budget experiment nonscanner instrument. *Rev. of Geophys.,* 24, 391-399.

Raval, A., and V. Ramanathan, 1989: Observational determination of the greenhouse effect. *Nature,* 342, 758-762.

Read, W. G., J. W. Waters, D.A. Flower, L. Froidevaus, R. F. Jarnot, D. L. Hartmann, R. S. Harwood, and R. G. Rood, 1995: Upper tropospheric water vapor from UARS MLS. *Bull.* Am. *Meteorol. Sot.,* 76,2381-2389.

Reynolds, R. W., and T. M. Smith, 1995: A high-resolution global sea surface temperature climatology. *J. Climate, 8,* 1571-1583.

Rossow, W. B., and R. A. Schiffer, 1991: ISCCP cloud data product. *Bull. Amer. Meteor. Sot.,* 72, 1-20.

Soden, B. J., and R. Fu, 1995: A satellite analysis of deep convection, upper-tropospheric humidity, and the greenhouse effect. *J. Climate,* 8,2335-2351.

Stone, E. M., W. J. Randel, J. L. Stanford, W. G. Read, J. W. Waters, 1996: Baroclinic wave vari-ations observed in MLS upper tropospheric water vapor. *Geophys. Res. Lett.,* 23, 2967-2970.